Dilute random-field Ising models and uniform-field antiferromagnets

Amnon Aharony
Department of Physics and Astronomy, Tel Aviv University, 69978 Tel Aviv, Israel

A. Brooks Harris
Department of Physics, University of Pennsylvania, Philadelphia, Pennsylvania 19104

Yigal Meir
Department of Physics and Astronomy, Tel Aviv University, 69978 Tel Aviv, Israel

The order-parameter susceptibility χ of dilute Ising models with random fields and dilute antiferromagnets in a uniform field are studied for low temperatures and fields with use of low-concentration expansions, scaling theories, and exact solutions on the Cayley tree to elucidate the behavior near the percolation threshold at concentration p_c. On the Cayley tree, as well as for $d > 6$, both models have a zero-temperature susceptibility which diverges as $|\ln(p_c - p)|$. For spatial dimensions $1 < d < 6$, a scaling analysis shows that the susceptibilities of the two models exhibit the same divergence, $\chi \sim (p_c - p)^{-(\gamma_p - \beta_p)/2}$, where γ_p and β_p are percolation exponents associated with the susceptibility and order parameter. At $d = 6$, the susceptibilities diverge as $|\ln(p_c - p)|^{9/7}$. For $d = 1$, exact results show that the two models have different critical exponents at the percolation threshold. The (finite-length) series at $d = 2$ seems to exhibit different critical exponents for the two models. At $p = p_c$, the susceptibilities diverge in the limit of zero field h as $\chi \sim h^{-(\gamma_p - \beta_p)/(\gamma_p + \beta_p)}$ for $d < 6$, as $\chi \sim |\ln h|^{9/7}$ for $d = 6$, and as $\chi \sim |\ln h|$ for $d > 6$.

I. INTRODUCTION

The critical properties of magnets are drastically affected by the presence of *random magnetic fields*.[1] In particular, theory shows that their equilibrium states are strongly modified by random fields: Their critical exponents deviate from their mean-field values at an upper critical dimension d_c, whose value is 6 instead of 4 as in the absence of such fields, and the lower critical dimension d_l, below which long-range order is destroyed by thermal fluctuations has the value 4 for $n \geq 2$ spin components, instead of 2,[2] and $d_l = 2$ for the Ising model ($n = 1$), instead of 1.[2-11] Recently, it has been shown that the observable behavior at low temperatures results from a metastable freezing of domains.[5,6]

The best experimental realization of a random-field Ising model (RFIM) has been the *dilute antiferromagnet in a uniform field* (DAFF). Fishman and Aharony[7] showed that in the presence of a uniform field the random exchange interactions give rise to local random staggered fields. Similar terms are generated by the randomness in the magnetic moments.[8-10] In the case of dilution, these local staggered fields are generated in any antiferromagnetic unit cell which has an unequal number of sites on the two sublattices. Assuming a finite macroscopic concentration of such unit cells, the DAFF is expected to exhibit the same critical behavior as the RFIM. Indeed, many recent experiments on DAFF's have confirmed some of the theoretical predictions derived for the RFIM.[11] Since the assumption that these two models, the RFIM and the DAFF, have the same critical behavior has

such important consequences, we felt that a detailed analysis of the correspondence between these two models was appropriate.

Most of the theoretical and experimental emphasis so far has been on the random-field-temperature ($h - T$) phase diagram for low-dilution systems. A critical line $h_c(T)$ separates the paramagnetic phase from the low-temperature ordered phase. Since long-range order is thermally unstable for $d \leq d_l$ one has that $h_c(T) = 0$ for $d \leq d_l$. However, finite-sized domains may show local ordering for $h < \tilde{h}_c(T)$, where the limiting field for metastability, $\tilde{h}_c(T)$, is larger than $h_c(T)$.[11] Also nonequilibrium hysteretic effects arise for h less than some limiting field $\tilde{h}_c$. Near the critical temperature of the "pure" system, T_c, all these critical fields have the asymptotic form,[7,12] $h_c(T) \sim (T_c - T)^{\gamma/2}$, where γ is the susceptibility exponent of the pure system.

In the dilute case one introduces another parameter, i.e., the concentration p of magnetic ions which are quenched into random sites on the lattice. The phase diagram must therefore be studied in the *three*-dimensional space of the variables, h, T, and p. Although randomness in the exchange interactions is technically irrelevant near the fixed point characterizing the RFIM behavior[12] (at least when the specific heat of the RFIM does not diverge), it will certainly have drastic effects near the *percolation threshold* at p_c, where the critical surface $h_c(T,p)$ must approach zero. At $T = 0$, it has been shown[13] that the critical line has the shape $h_c \sim (p - p_c)^{(\gamma_p + \beta_p)/2}$, where $(p - p_c)^{\beta_p}$ is proportional to the probability that a site

belongs to the infinite percolating cluster, and $(p-p_c)^{-\gamma_p}$ describes the mean size of the finite clusters. At higher fields, the infinite cluster breaks into domains of size $\xi \sim |p-p_c|^{-\nu_p}$, where ξ is the percolation correlation length and ν_p the associated critical exponent.[13] In fact, one expects a series of fields above h_c at which groups of spins will find it favorable to flip into the direction of their local net random field.[14] Traces of such transitions may have been observed in recent experiments.[15,16]

The expected $h-T-p$ phase diagram for $d>d_l$ is shown schematically in Fig. 1. Note that since[17] $\beta_p+\gamma_p \approx 1.2$ for $d=3$, the critical line approaches the p axis tangentially at $T=0$ (in contrast to approaching it with infinite slope at T_c, where $\gamma<2$). The line $h_c(T,p)$ for fixed p is thus expected to decrease to zero rather quickly as $p \to p_c$. Some of the experiments which exhibited no long-range order at finite values of h may have simply explored the region above this line! For $d=2$, h_c is zero for $p<1$. However, the nonequilibrium surface $\tilde{h}_c$ is expected to have a similar behavior as shown in Fig. 1 with[17] $\beta_p+\gamma_p \approx 2.53$. In the present paper we study the critical properties of both the RFIM and the DAFF in the vicinity of the percolation threshold at $p=p_c$, $T=0$. Strictly speaking, a comparison of the two models for $T=0$ and $p \to p_c$ is not equivalent to a comparison of their critical behaviors along a path for which p is constant $(p>p_c)$ and $T \to T_c(p)$. However, the present work is the first detailed calculation which elucidates the relation between the two models and our conclusions concerning the transitions at $T=0$ probably also apply to the transition which occurs for $p>p_c$, when $T \to T_c(p)$. Nevertheless, to emphasize this distinction we will refer to the diluted RFIM for $p \to p_c$ at $T=0$ as the DRFIM.

At $T=0$, the system at equilibrium is frozen into one of its ground states. The nature of this state changes from ferromagnetic, for $h<h_c$, to a domain state for $h>h_c$. This domain state probably persists at all fields for $p>p_c$. As p is increased at fixed $h>0$, the system first goes into the domain state, at $p=p_c$, and then (for $d>d_l$) becomes ferromagnetic when $h_c(p)$ becomes equal to h.

For high spatial dimension the critical behavior is essentially the same as that for the Cayley tree where we give an exact analysis. We present a scaling analysis using

our knowledge of the form of the cluster distribution for percolation for p near p_c. In addition, we calculate the order-parameter susceptibility χ for these models as an expansion in powers of p for small, but nonzero h, and fit our results to the expected asymptotic critical form, viz.,

$$\chi \sim (p_c-p)^{-\gamma} , \qquad (1.1)$$

to obtain the critical exponent γ for each model. Here χ is actually defined [in Eq. (2.2), below] as T/μ^2 times the susceptibility, where μ is the magnetic moment of a single spin. The result (1.1) applies when the measured values are extrapolated to $T=0$.

At high dimensions, $d \geq 3$, we conclude that $\gamma_{DRFIM}=\gamma_{DAFF}$, as expected. Our scaling analysis indicates that this exponent is equal to $(\gamma_p-\beta_p)/2$. For $d \geq 6$, the divergence in χ becomes logarithmic. The divergence of χ at infinitesimally small h is thus drastically different from that of the zero-field susceptibility, which diverges as $(p_c-p)^{-\gamma_p}$. The exponent γ thus shows a discontinuous jump as $h \to 0$.

At $d=1$ we find $\gamma_{DRFIM}=\frac{1}{2}$, while $\gamma_{DAFF}=\gamma_p=1$. The fact that γ_{DAFF} differs from γ_{DRFIM} and is equal to γ_p is a consequence of the negligibly small concentration of random staggered fields generated in the DAFF case. (For $d=1$ these random fields only occur at the end of the finite chains.) Although this concentration is expected to be finite for $d>1$, our series analysis seems to yield $\gamma_{DRFIM}>\gamma_{DAFF}$ at $d=2$. If not a transient crossover effect, this would imply that the two models are different at $d=2$.

The outline of this paper is as follows: The Hamiltonians and the susceptibilities for the various models are defined and generally discussed in Sec. II. Scaling arguments for the critical exponents of the models considered are given in Sec. III. Section IV contains an exact evaluation of χ for each model at $d=1$, and an exact evaluation of χ on a Cayley tree is given in Sec. V. Similar results are reproduced for $d>6$ using the field-theoretical approach to percolation in Sec. VI, where the behavior of χ for $d=6$ and $d=6-\epsilon$ is also analyzed. Low concentration series for these χ's are derived and analyzed in Sec. VII. Section VIII contains our conclusions. In Appendix A we show how the distribution function for sublattice occupation for percolation can be obtained from a Potts model in a staggered field.

II. DEFINITIONS AND GENERAL EXPRESSIONS FOR SERIES

Our analysis starts from the site-diluted Ising ferromagnet, whose Hamiltonian is

$$H=-J\sum_{\langle ij \rangle} t_i t_j S_i S_j - \sum_i h_i t_i S_i , \qquad (2.1)$$

where $S_i=\pm 1$ are the Ising spins, $\langle ij \rangle$ denotes pairs of nearest neighbors, $J>0$ is the exchange constant, and t_i is a random-site occupation variable, equal to 1 with probability p and 0 with probability $1-p$. A similar Hamiltonian may be written for bond dilution. We will treat the case of quenched randomness, in which case the relevant free energy is the free energy of the above model averaged
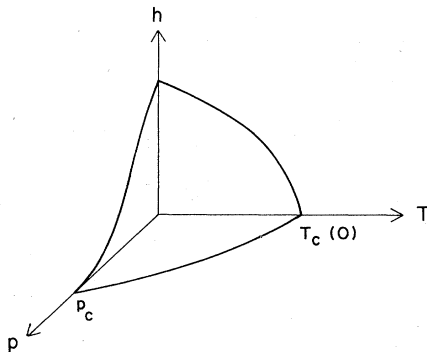
FIG. 1. Phase diagram in the random-field—concentration—temperature space.

over its random configurations, as discussed below. For the DRFIM, the fields h_i are random, assuming the values $+h$ and $-h$ with equal probability. The Hamiltonian for the DAFF may be mapped onto that of Eq. (2.1), by changing the signs of all spins S_i on one of the sublattices. A uniform field (on the DAFF) is thus equivalent to a staggered field (on the dilute ferromagnet), i.e., $h_i = h$ on one sublattice and $h_i = -h$ on the other. In the following we will always discuss the DAFF in its representation as a dilute ferromagnet in a staggered field. Thus both models are dilute ferromagnets. For the DRFIM each h_i is random in sign, whereas for the DAFF each h_i assumes its value for a nonrandom, but staggered, field. In both cases $|h_i| = h$.

The order-parameter susceptibility (in units of μ^2/T) is defined via

$$\chi = \sum_{i,j} [\langle S_i S_j \rangle - \langle S_i \rangle \langle S_j \rangle]_c , \qquad (2.2)$$

where $\langle \ \rangle$ denotes a thermal average, which at $T=0$ becomes an average over the degenerate ground states, and $[\ ]_c$ indicates a configurational average over the random variables t_i and h_i. At low concentration, there exist only finite clusters, and χ may be calculated as the sum of the susceptibilities of each cluster:

$$\chi = N \sum_{\Gamma} P(\Gamma)\chi(\Gamma) , \qquad (2.3)$$

where $P(\Gamma)$ is the average number of clusters per site of type Γ, N is the total number of sites, and $\chi(\Gamma)$ is given by Eq. (2.2) with i and j running over the sites of Γ.

At $h=0$ all spins on a cluster Γ are parallel to each other in the ground state, so that $\langle S_i S_j \rangle = 1$. Since there are two signs of S_i, there are two degenerate ground states and $\langle S_i \rangle = 0$. Thus, $\chi(\Gamma) = n_{\Gamma}^2$, where n_{Γ} is the number of sites in the cluster Γ. Since $\chi(\Gamma)$ is a function only of n_{Γ}, we can express χ in terms of the distribution function $W(n;p)$, defined to be the average number of clusters per site consisting of n sites: $W(n;p) = \sum_{\Gamma} P(\Gamma)\delta_{n,n_{\Gamma}}$, where δ is the Kronecker delta. The susceptibility at $h=0$ is the usual ferromagnetic (FM) one,

$$\chi_{\text{FM}} = N \sum_{\Gamma} P(\Gamma) n_{\Gamma}^2 = N \sum_n W(n;p)n^2 ,$$

which diverges for $p \to p_c$ as $|p_c - p|^{-\gamma_p}$.[17]

In the other extreme limit, $h \gg J$, every spin S_i is oriented along h_i: $S_i = \text{sgn}h_i$. The ground state is therefore nondegenerate, so that $\langle S_i S_j \rangle = \langle S_i \rangle \langle S_j \rangle = \text{sgn}(h_i h_j)$, and $\chi = 0$. As we lower the field, groups of spins may flop and order ferromagnetically.[14] These groups become larger as h decreases. For any finite cluster, Γ, there exists a sufficiently low field h_{Γ} below which all the spins on the cluster are parallel to each other. The value of h_{Γ} is easily estimated by noting that the net field energy of a large ferromagnetic cluster is of order $hn_{\Gamma}^{1/2}$, whereas the price to break the cluster into domains (provided the linear size of the cluster is smaller than the percolation correlation length, ξ, as practically all finite clusters for $p < p_c$ are) is of order J.[13] The cluster may thus break into domains when $n_{\Gamma} > (J/h)^2$. (Note that this is correct at *all* dimensions.) The sum in Eq. (2.3) should

thus be cut off at $n_c(h) \sim (J/h)^2$. For $n_{\Gamma} < n_c(h)$, the whole cluster consists of a single ferromagnetic domain, with all S_i's having the same sign. In the following we first evaluate the sum in Eq. (2.3) for very small finite values of h, letting the cutoff $n_c(h)$ be infinite. It is interesting to note that the limit $h \to 0$ yields results which are different from χ_{FM} calculated at $h=0$.

We now concentrate on clusters with $n_{\Gamma} < n_c(h)$. Consider a cluster on which there is a net magnetic field, i.e., $\sum_i h_i \neq 0$. Clearly, the ground state of this cluster will be nondegenerate with all spins having the same sign as the net field. Thus, $\langle S_i S_j \rangle = \langle S_i \rangle \langle S_j \rangle = 1$, and $\chi(\Gamma) = 0$. For fields $\pm h$, this will happen for all the clusters with an *odd* number of spins, i.e., for n_{Γ} odd. Many of the clusters with n_{Γ} even will also have a net field, and thus will not contribute to χ. Only the clusters with n_{Γ} even and which have an equal number of $h_i = h$ and $h_i = -h$ will contribute. These clusters will have doubly degenerate ground states, and therefore $\langle S_i S_j \rangle = 1$, $\langle S_i \rangle = 0$, and $\chi(\Gamma) = n_{\Gamma}^2$. The calculation of χ thus reduces to the counting of these clusters. This counting is different for the DRFIM and the DAFF.

For the DRFIM, the probability that exactly k out of $n_{\Gamma} = 2k$ sites have $h_i = +h$ is $(\frac{1}{2})^{2k}\binom{2k}{k}$, where $\binom{m}{n}$ denotes $m!/[n!(m-n)!]$. Thus we have

$$\chi_{\text{DRFIM}} = N \sum_{\Gamma: \ n_{\Gamma}=2k} P(\Gamma)2^{-2k}\binom{2k}{k}(2k)^2 \qquad (2.4a)$$

$$= N \sum_k W(2k;p)2^{-2k}\binom{2k}{k}(2k)^2 . \qquad (2.4b)$$

For the DAFF, the sum in Eq. (2.3) will be limited to those clusters on which the numbers of sites on the two sublattices A and B (denoted n_A and n_B, respectively) are equal, $n_A = n_B = k = n_{\Gamma}/2$, so that

$$\chi_{\text{DAFF}} = N \sum_{\Gamma: \ n_A=n_B} P(\Gamma)n_{\Gamma}^2 . \qquad (2.5a)$$

Here it is convenient to express the result in terms of a distribution function $W(n_A,n_B;p)$ defined to be the average number of clusters per site consisting of n_A sites on the A sublattice and n_B sites on the B sublattice. Then Eq. (2.5a) becomes

$$\chi_{\text{DAFF}} = N \sum_k W(k,k;p)(4k^2) . \qquad (2.5b)$$

So far, we have discussed only the susceptibility χ. Neutron scattering experiments usually measure the wave-vector-dependent structure factor, $S(\mathbf{q})$, which is the spatial Fourier transform of $[\langle S_i S_j \rangle]_c$. At zero wave vector, one has

$$S(0) = \sum_{i,j} [\langle S_i S_j \rangle]_c = \sum_{\Gamma} P(\Gamma)S(0,\Gamma) . \qquad (2.6)$$

where $S(0,\Gamma)$ is the structure factor at zero wave vector for the cluster Γ. In the limit $h \to 0$, all the spins in the ground state are parallel to each other, $\langle S_i S_j \rangle = 1$, and we find that

$$S(0) = N \sum_{\Gamma} P(\Gamma)n_{\Gamma}^2 = \chi_{\text{FM}} = N \sum_n W(n;p)n^2 . \qquad (2.7)$$

For large h, $S_i = \mathrm{sgn} h_i$, and $\langle S_i S_j \rangle = \mathrm{sgn} h_i h_j$, so that the configurational average $[\langle S_i S_j \rangle]_c$ will vanish. Again, the sum in Eq. (2.7) will have to be cut off at $n_\Gamma = n_c(h)$.

III. SCALING ANALYSIS FOR THE DRFIM AND THE DAFF

In this section we give *scaling* arguments for the susceptibilities of the DRFIM and DAFF. First we consider the DRFIM and note that Eq. (2.4) for $\mathcal{X}_{\mathrm{DRFIM}}$ amounts to calculating the (even) cluster average of $(\frac{1}{2})^{2k} \binom{2k}{k}(2k)^2$. Simple identities[18] turn this into

$$2^{-2k}\binom{2k}{k}(2k)^2 = \frac{4}{\sqrt{\pi}} \frac{k \Gamma(k+\frac{1}{2})}{\Gamma(k)}$$

$$\approx \frac{4}{\sqrt{\pi}} k^{3/2}\left[1 + O\left[\frac{1}{k}\right]\right] . \quad (3.1)$$

Thus the asymptotic behavior of $\mathcal{X}_{\mathrm{DRFIM}}$ is the same as that of $\sum_n W(n,p)n^{3/2}$. For large n, the average number of clusters per site, $W(n,p)$ may be written in the scaling form[17]

$$W(n,p) = n^{-\tau} f(n^\sigma(p_c - p)) , \quad (3.2)$$

where f is a scaling function. From this result one easily reproduces the relations $\gamma_p = (3-\tau)/\sigma$ (from the average of n^2) and $\beta_p = (\tau - 2)/\sigma$ (from the average of n). Thus, we find that

$$\gamma_{\mathrm{DRFIM}} = (\tfrac{5}{2} - \tau)/\sigma = (\gamma_p - \beta_p)/2 . \quad (3.3)$$

Equation (3.2) was first given by Stauffer based on heuristic arguments. It was later verified by Stephen[19] within by a renormalization-group expansion in $6 - \epsilon$ dimensions. More recently Harris and Lubensky[20] have reexamined this problem in order to discuss how $W(n;p)$ crosses over from percolation behavior for $n^\sigma(p_c - p)$ of order unity to the behavior of lattice animals[21] for large values of this variable. In particular, Eq. (3.2) is incorrect for $6 < d < 8$. However, we will only be concerned here with convolutions of $W(n;p)$ with powers of n, and these quantities are essentially determined by the behavior of $W(n;p)$ for $n^\sigma(p_c - p)$ of order unity. In this regime the results of Ref. 20 indicate that deviations from Eq. (3.2) are unimportant.

At a finite field (i.e., for $h/J \ll 1$) the various sums must be cut off at $n_c(h) \sim (J/h)^2$. Using Eq. (3.2), we deduce that

$$\mathcal{X}_{\mathrm{DRFIM}} = (p_c - p)^{-(\gamma_p - \beta_p)/2} X([n_c(h)]^\sigma(p_c - p))$$

$$= (p_c - p)^{-(\gamma_p - \beta_p)/2} \widetilde{X}(h^2/(p_c - p)^\varphi) , \quad (3.4)$$

where X and $\widetilde{X}$ are scaling functions and $\varphi = 1/\sigma = \beta_p + \gamma_p$.[13] As $h \to 0$, or $n_c(h) \to \infty$, the functions X and $\widetilde{X}$ approach constant values, and we recover Eq. (3.3). Note that the susceptibility in this limit differs from that of a dilute ferromagnet, $\mathcal{X}_{\mathrm{FM}} \sim (p_c - p)^{-\gamma_p}$ expected *at* $h=0$. Equation (3.4) should thus be used only for $0 < h \ll J$, and a discontinuity is predicted as $h \to 0$. To treat this discontinuity in more detail would require introducing a scaling variable to describe the crossover with

respect to the temperature, which we have omitted here.

For finite h [or $n_c(h)$], $\mathcal{X}$ is expected to remain finite at p_c. The function $X(x)$ must therefore behave as a power of x for $x \to 0$: $X \sim x^{(\gamma_p - \beta_p)/2}$, and we find

$$\mathcal{X}_{\mathrm{DRFIM}} = [n_c(h)]^{\sigma(\gamma_p - \beta_p)/2} \sim h^{-(\gamma_p - \beta_p)/(\gamma_p + \beta_p)}$$

$$\text{for } p_c - p \ll [n_c(h)]^{-\sigma} \sim (h/J)^{2/(\gamma_p + \beta_p)} . \quad (3.5)$$

An exception will occur for $d=1$, as discussed in the next section.

Results like Eqs. (3.4) and (3.5) also apply for the other quantities. In particular, in the same regime of validity as Eq. (3.5) we have

$$S(0) \sim h^{-2\gamma_p/(\gamma_p + \beta_p)} . \quad (3.6)$$

For the DAFF, Eq. (2.5) requires knowledge of the probability that a cluster of n sites have exactly $n_A = n_B = n/2$ sites on each sublattice. For large n, it is reasonable to expect that the probability of adding one more site to sublattice A is equal to that of adding one to sublattice B. Thus, the variable $n_A - n_B$ grows in equally probable steps of $+1$ or -1, exactly as in a one-dimensional random walk. After $n = n_A + n_B$ such steps, the distribution function of $n_A - n_B$ is thus

$$W(n_A, n_B; p)/W(n;p) = 2(\pi a n)^{-1/2} e^{-(n_A - n_B)^2/(an)} , \quad (3.7)$$

where a depends on p. The probability to have $n_A = n_B$ after n steps is thus of order $(n)^{-1/2}$. (A similar argument has been used by Harris and Kirkpatrick[22] to discuss the Heisenberg version of the DAFF.) Substituting into Eq. (2.5) we obtain the relation

$$\mathcal{X}_{\mathrm{DAFF}} \sim N \sum_{n \text{ even}} W(n,p)n^{3/2} , \quad (3.8)$$

which is the same as $\mathcal{X}_{\mathrm{DRFIM}}$ from Eq. (3.1).

Appendix A contains a derivation of Eq. (3.7) based on a mean-field treatment of the free energy of the $s=1$ state Potts model and an argument giving a generalization beyond mean-field theory.

IV. ONE DIMENSION

In one dimension, all the finite clusters are chain segments. The probability of finding a cluster of exactly n sites is thus $p^n(1-p)^2$, where p is the concentration of sites or $p^{n-1}(1-p)^2$, if p denotes the bond concentration. Clearly, both will yield the same critical behavior. Using the former, we have for a dilute ferromagnet

$$\mathcal{X}_{\mathrm{FM}}/N = \sum_{n=1}^{\infty} (1-p)^2 p^n n^2$$

$$= p(p+1)/(1-p) \approx 2/(1-p) , \quad (4.1)$$

i.e., $p_c = 1$ and $\gamma_p = 1$.

In this special case, *all* the clusters with even n will have $n_A = n_B = k = n/2$. Thus

$$\chi_{\text{DAFF}}/N = \sum_{k=1}^{\infty} (1-p)^2 p^{2k}(2k)^2$$

$$= \frac{4p^2(p^2+1)}{(p+1)^3(1-p)} \approx 1/(1-p) , \qquad (4.2)$$

i.e., $\gamma_{\text{DAFF}} = \gamma_p = 1$.

Note that the field on a typical unit cell with sites labeled 1 and 2 is[8] [see Eq. (2.1)]

$$h(S_1 t_1 - S_2 t_2) = \tfrac{1}{2} h[(S_1 - S_2)(t_1 + t_2)$$

$$+ (S_1 + S_2)(t_1 - t_2)] , \qquad (4.3)$$

implying a net local field (coupled to the ferromagnetic order parameter $S_1 + S_2$) only when $t_1 - t_2 \neq 0$, i.e., when $t_1 = 1$, $t_2 = 0$, or $t_2 = 1$, $t_1 = 0$. This occurs only at the *edges* of the cluster. For very large clusters, the weight of the edges becomes negligible and therefore we reproduce the critical behavior of the zero-field ferromagnet. Note, however, that the amplitude for the DAFF is half as large as for the FM.

We now turn to the DRFIM. Here, using Eq. (2.8), we have

$$\chi_{\text{DRFIM}}/N = \sum_{k=1}^{\infty} (1-p)^2 (p/2)^{2k} \binom{2k}{k}(2k)^2$$

$$\approx \frac{4}{\sqrt{\pi}}(1-p)^2 \sum_{k=1}^{\infty} \frac{k\Gamma(k+\tfrac{1}{2})}{\Gamma(k)} p^{2k} . \qquad (4.4)$$

For large k, the ratio of successive coefficients in Eq. (4.4) is

$$a_{k+1}/a_k = (k+1)(k+\tfrac{1}{2})/k^2 \approx 1 + \frac{3}{2k} , \qquad (4.5)$$

from which we identify the asymptotic behavior of the sum as $(1-p)^{-5/2}$. Thus we have

$$\chi_{\text{DRFIM}}/N \sim (1-p)^{-1/2} , \qquad (4.6)$$

and $\gamma_{\text{DRFIM}} = \tfrac{1}{2}$. Noting that[17] $\gamma_p = 1$ and $\beta_p = 0$, we see that this agrees with the general result stated in Eq. (3.3). Thus for $d=1$, the DRFIM behaves differently from the DAFF, the latter being similar to the FM!

As noted, Eq. (4.6) applies only for $h \to 0$. At finite h, we must cut off the sum in Eq. (4.4) at $2k \sim n_c(h) \sim (J/h)^2$. Approximating the coefficient inside the sum by $k^{3/2}$, and the sum by an integral, we have[18]

$$\chi_{\text{DRFIM}}/N \sim (1-p)^2 \int_0^{n_c(h)} dx \, x^{3/2} e^{-2x \, |\ln p|}$$

$$\sim (1-p)^2 |\ln p|^{-5/2} \gamma[\tfrac{5}{2}, 2n_c(h)|\ln p|] , \qquad (4.7)$$

where γ is the incomplete gamma function. Using[18]

$$\gamma(5/2, y) = \frac{3}{4} \sqrt{\pi} \Phi(\sqrt{y}) - (y^{3/2} + \tfrac{3}{2} y^{1/2}) e^{-y} , \qquad (4.8)$$

where Φ is the probability integral,

$$\Phi(\sqrt{y}) \to \begin{cases} 1, & y \gg 1 \\ \dfrac{2}{\sqrt{\pi}} \sqrt{y} , & y \ll 1 \end{cases} \qquad (4.9)$$

and $|\ln p| \approx 1 - p$, we find

$$\chi_{\text{DRFIM}}/N \to \begin{cases} (1-p)^{-1/2}, & 1-p \gg (h/J)^2 \\ (1-p)(J/h)^3, & 1-p \ll (h/J)^2 . \end{cases} \qquad (4.10)$$

Thus, as a function of p, the susceptibility will have a peak at $1-p \sim (h/J)^2$, and then decrease linearly to zero as $p \to 1$ at fixed h, with slope of order h^{-3}.

Equation (4.7) is a special example of the scaling form of Eq. (3.4), with $\varphi = 1/\sigma = 1$. However, unlike Eq. (3.5), χ_{DRFIM} does not approach a finite value at $p_c = 1$. Instead, χ_{DRFIM} vanishes, linearly in $(1-p)$, simply because there are no finite clusters left at $p = 1$. The second limit in Eq. (4.10) may still be derived from Eq. (3.4) if one lets $X(x)$ vanish as $x^{3/2}$.

We finally turn to the structure factor at zero wave vector. Truncating the sum in Eq. (3.4) at $n_c(h)$ we find, by a similar calculation,

$$S(0) \to \begin{cases} (1-p)^{-1}, & 1-p \gg (h/J)^2 , \\ (1-p)^2(J/h)^6, & 1-p \ll (h/J)^2 . \end{cases} \qquad (4.11)$$

V. EXACT RESULTS FOR THE CAYLEY TREE

In this section we will give exact calculations for the models we have considered on the site diluted Cayley tree. The Cayley tree is a hierarchical lattice with no loops, in which each vertex has $\sigma + 1$ neighboring vertices. For the limiting case, $\sigma = 1$ the Cayley tree is a linear chain.

We first consider the random-field model. We make an explicit evaluation of Eq. (3.4), for which we used the exact solution[23] for the average number of clusters of n sites:

$$W(n;p) = (\sigma+1)(1-p)^2 \frac{(n\sigma)!}{n!(n\sigma-n+2)!}[p(1-p)^{\sigma-1}]^n . \qquad (5.1)$$

Then Eq. (2.4) yields

$$\chi_{\text{DRFIM}}/N = \frac{\sigma+1}{\sigma^2}(1-p)^2 \sum_{n=1}^{\infty} \frac{(2n\sigma)!}{n!n!(2n\sigma-2n)!} \left[\frac{p(1-p)^{\sigma-1}}{2}\right]^{2n} \left[\frac{2n\sigma}{2n\sigma-2n+1}\right] \left[\frac{2n\sigma}{2n\sigma-2n+2}\right] . \qquad (5.2)$$

To obtain the singular part of this expression we need only treat the terms for large n correctly. Thus, we have approximately

$$\chi_{\text{DRFIM}}/N \approx \frac{\sigma+1}{(\sigma-1)^2}(1-p)^2 \sum_{n=1}^{\infty} \frac{(2n\sigma)!}{n!n!(2n\sigma-2n)!} \left[\frac{p(1-p)^{\sigma-1}}{2}\right]^{2n} . \qquad (5.3)$$

Similarly we may now approximate all the factorials using Stirlings formula, whence

$$\chi_{\text{DRFIM}}/N \sim \frac{\sigma^{1/2}(\sigma+1)(1-p)^2}{2\pi(\sigma-1)^{5/2}} \sum_{n=1}^{\infty} \frac{1}{n} \left[\frac{\sigma^{\sigma} p (1-p)^{(\sigma-1)}}{(\sigma-1)^{(\sigma-1)}} \right]^{2n} , \tag{5.4}$$

$$\sim \frac{\sigma^{1/2}(\sigma+1)(1-p)^2}{2\pi(\sigma-1)^{5/2}} | \ln(1-x^2) | , \tag{5.5}$$

where

$$x = p\sigma[(1-p)/(1-\sigma^{-1})]^{(\sigma-1)} . \tag{5.6}$$

We wish to evaluate this for p near p_c. Therefore we write

$$t = (p_c - p)/p_c \rightarrow p = (1-t)/\sigma . \tag{5.7}$$

For small t we find that $x = 1 - at^2$, where a is an unimportant constant. Equation (5.5) then becomes

$$\chi_{\text{DRFIM}}/N \sim \frac{1+\sigma^{-1}}{\sigma\pi(1-\sigma^{-1})^{1/2}} | \ln t | . \tag{5.8}$$

The approximations we have made are appropriate for $\sigma > 1$. For $\sigma = 1$ the solution is that for $d = 1$ given above.

We now consider the DAFF. We first introduce generating functions $F_{\pm}(\alpha,x,p)$ to describe clusters grown from an origin on the A sublattice (for F_+) or the B sublattice (for F_-). In these generating functions we will associate a factor αx with occupied A sites and α/x with occupied B sites. We write

$$F_{\pm} = \alpha p x^{\pm 1} \Phi_{\pm}^{\sigma+1}(\alpha,x,p) , \tag{5.9}$$

where the "branch" functions $\Phi_{\pm}$ satisfy the recursion relation

$$\Phi_{\pm}(\alpha,x,p) = 1 - p + \alpha p x^{\mp 1} \Phi_{\mp}(\alpha,x,p)^{\sigma} . \tag{5.10}$$

Thus Φ_+, for instance, is the solution to

$$\Phi_+(\alpha,x,p) = 1 - p + (\alpha p/x)[1 - p + \alpha p x \Phi_+(\alpha,x,p)^{\sigma}]^{\sigma} . \tag{5.11}$$

The recursion relation, Eq. (5.10), expresses the fact that

at any stage a neighboring site can be absent (with probability $1-p$) or present (with probability p), in which case it carries a factor $\alpha x^{\mp 1}$ for the added site and $\Phi_{\mp}$ for each of the σ additional branches. Note that averages of powers of n_{Γ} can be generated by suitable derivatives with respect to α. Also, since each cluster is weighted by the factor $x^{n_A - n_B}$, $F_{\pm}$ contains information about the distribution of $n_A - n_B$. In fact we can express the susceptibility as

$$\chi_{\text{DAFF}}/N = \frac{1}{2\pi i} \int \frac{dx}{x} \frac{\partial}{\partial\alpha} F_+(\alpha,x,p) \bigg|_{\alpha=1} . \tag{5.12}$$

Here the contour integral over x picks out the term of order x^0 which reproduces the constraint $n_A = n_B$ in Eq. (2.5). One factor of n_{Γ} comes from the derivative with respect to α and the other comes from the fact that any given cluster can be realized n_{Γ} times by growing clusters, since any site in the cluster could be the origin of growth. One would naturally write Eq. (5.12) with $(F_+ + F_-)/2$ appearing in place of F_+. However, since the contributions from F_+ and F_- are equal by symmetry, we use the more convenient form of Eq. (5.12) as written.

Superficially it looks as though we need to solve Eq. (5.11) to obtain an explicit representation for χ_{DAFF}. We avoid this problem by using the identity

$$\frac{1}{2\pi i} \int t^k \frac{F'(t)}{F(t)} dt = t_0^k \tag{5.13}$$

where it is assumed that $F(t)$ has a single zero inside the contour of integration at $t = t_0$. Thus we write

$$\int t^{\sigma+1} \frac{1 - (\alpha\sigma p)^2 t^{\sigma-1}(1-p+\alpha p x t^{\sigma})^{\sigma-1}}{t - 1 + p - \dfrac{\alpha p}{x}(1-p+\alpha p x t^{\sigma})^{\sigma}} \frac{dt}{2\pi i} = [\Phi_+(\alpha,p,x)]^{\sigma+1} , \tag{5.14}$$

since the zero of the denominator yields the solution to Eq. (5.11). Substituting this representation into Eq. (5.12) we obtain an expression for χ_{DAFF} as a double (contour) integral over t and x. It is convenient to expand the integrand as an infinite series in inverse powers of $(t - 1 + p)$ and interchange the order of integrations. Also we set $u = t/(1-p)$ and $\beta = \alpha p (1-p)^{\sigma-1}$, in terms of which variables we have

$$\chi_{\text{DAFF}}/N = (1-p)^{\sigma+1} \frac{\partial}{\partial\beta} \beta \sum_{l=0}^{\infty} \int \frac{du}{2\pi i} \frac{u^{\sigma+1}}{(u-1)^{l+1}} \int \frac{dx}{2\pi i} \left[\frac{\beta}{x} \right]^l (1+\beta x u^{\sigma})^{\sigma l}[1 - \beta^2 \sigma^2 u^{\sigma-1}(1+\beta x u^{\sigma})^{\sigma-1}] , \tag{5.15}$$

where this expression is to be evaluated at $\beta = p(1-p)^{\sigma-1}$. This series can be integrated term by term first over x and then over u, whence we obtain the remarkably compact result

$$\chi_{\text{DAFF}}/N = 2(\sigma+1)(1-p)^2 \sum_{l=1}^{\infty} [p(1-p)^{(\sigma-1)}]^{2l} \begin{bmatrix} \sigma l \\ l-1 \end{bmatrix}^2 .$$

$$(5.16)$$

To obtain the asymptotic form for χ_{DAFF} for p near p_c we proceed as before: We use approximations which are asymptotically correct for large l, especially Stirling's approximation for the factorial. The calculation is straightforward and similar to that for χ_{DRFIM}, so we only quote the result

$$\chi_{\text{DAFF}}/N \sim \frac{2(1+\sigma^{-1})}{\pi\sigma(1-\sigma^{-1})} |\ln t| ,$$

$$(5.17)$$

where t is as defined in Eq. (5.7).

Thus we see that both χ's have essentially the same critical behavior. It is interesting that we find a logarithmic singularity for the Cayley tree inasmuch as this result can be identified with mean-field theory. As we show below, the same result arises from the field-theoretical description of percolation for $d > 6$.

VI. BEHAVIOR NEAR SIX DIMENSIONS

As we have seen in Sec. III, the asymptotic behavior of χ_{DAFF} is the same as that of $\sum_n W(n;p)n^{3/2}$. Consequently, the singularity in χ_{DAFF} is determined by the large n behavior of $W(n;p)$. For $d < 6$ we have already carried out the scaling analysis of χ_{DAFF} based on the asymptotic form of the distribution function W in Eq. (3.2). These general results were indeed confirmed using the ϵ expansion of $W(n;p)$ in $d = 6 - \epsilon$ dimensions.[19,20]

At $d = 6$, the distribution function at $p = p_c$ becomes[24]

$$W(n;p) \sim |\ln n|^{2/7} n^{-5/2} ,$$

$$(6.1)$$

and thus

$$\chi_{\text{DRFIM}} \sim \sum_n W(n;p)n^{3/2}$$

$$\sim |\ln n_c(h)|^{9/7} \sim |\ln h|^{9/7} .$$

$$(6.2)$$

For $p < p_c$ one recovers the same results, with $n_c(h)$ replaced by $(p-p_c)^{-2}$, where we used the fact that $\beta + \gamma = 2 + O(\epsilon^2)$, i.e.,

$$\chi_{\text{DRFIM}} = |\ln(p_c - p)|^{9/7} .$$

$$(6.3)$$

For $d > 6$, the result for $p = p_c$ is[20,24] $W(n;p) \sim n^{-5/2}$ [see also Eq. (A15), for $n_s = 0$], so that $\chi_{\text{DRFIM}} \sim |\ln n_c(h)| \sim |\ln h|$. Extension of these results to $p < p_c$ is again accomplished by replacing $n_c(h)$ by $(p-p_c)^2$:

$$\chi_{\text{DRFIM}} \sim |\ln(p_c - p)| ,$$

$$(6.4)$$

in agreement with our result in Sec. V for the Cayley tree.

VII. SERIES IN d DIMENSIONS

We expect the same critical behavior if the clusters are generated by bond dilution or by site dilution (as long as n_Γ still denotes the number of *sites* on the cluster Γ). For convenience, we derived the series for the former, and p

denotes the concentration of nonzero bonds. The probability $P(\Gamma)$ is now given by[25]

$$P(\Gamma) = w_\Gamma(d)p^{b_\Gamma}(1-p)^{s_\Gamma} ,$$

$$(7.1)$$

where $w_\Gamma(d)$ is the weak embedding constant of Γ (which gives the number of occurrences per site of the diagram Γ and its topological equivalents on a d-dimensional hypercubic lattice), and b_Γ and s_Γ are, respectively, the number of occupied bonds in the cluster Γ and the number of vacant perimeter bonds defining the boundary of the cluster. Combining terms in the sum of Eq. (3.3) we may write[25]

$$\chi/N = \sum_\Gamma w_\Gamma(d)p^{b_\Gamma}\chi^c(\Gamma) ,$$

$$(7.2)$$

where $\chi^c(\Gamma)$ is the cumulant susceptibility of the diagram Γ defined recursively by

$$\chi^c(\Gamma) = \chi(\Gamma) - \sum_{\gamma \subset \Gamma} \chi^c(\gamma) ,$$

$$(7.3)$$

where $\chi(\gamma)$ is the (bare) susceptibility for the cluster γ, and the sum over γ runs over all subclusters, if any, of Γ.

Instead of using n_Γ^2 for the susceptibility of clusters, we used $n_\Gamma(n_\Gamma - 1)$, i.e., in Eq. (3.4) we used $2k(2k-1)$ instead of $(2k)^2$. This does not affect the asymptotic behavior of the series. Also, we note that the weak embedding constants are polynomials in d whose leading term is of order $d^{n_b(\Gamma)}$. As a result we may write the series for the susceptibility in the form

$$\chi(d,p) = \sum_k \left[\sum_{l=1}^{k} A_{kl}d^l \right] p^k .$$

$$(7.4)$$

The series up to order p^{11} for the two models considered are given explicitly in Appendix B.

We have derived Dlog Padé approximants for these series for $1 < d \leq 8$, and plotted the residue (i.e., the value of the exponent γ obtained thereby) versus the location of the pole (i.e., the value of p_c) for the various approximants. We have then estimated the value of γ at $p = p_c$, where for p_c we used the current best estimates.[17] The results of this procedure are summarized in Table I. Except for the DRFIM at $d = 2$, we fitted a straight line to those points corresponding to poles within ± 0.01 of p_c, and the quoted error bars give the range in which γ lies with a certainty of 95%. The DRFIM at $d = 2$ had only three points in the above range, and the estimate of γ_{DRFIM} in this case is based on the 23 points in the range $0.45 < p_c < 0.55$, most of which lie near $p_c \approx 0.46$, $\gamma \approx 0.5$.

For $d \geq 3$, the results are all consistent with the equality

$$\gamma_{\text{DAFF}} = \gamma_{\text{DRFIM}} ,$$

$$(7.5)$$

which was expected both by the heuristic arguments concerning the random fields generated by the uniform fields on the randomly diluted magnet[7] and by the scaling arguments presented above. As mentioned in the Introduction, our results offer the first quantitative calculational confirmation that the DAFF and the RFIM do, indeed, have the same critical exponents.

The last column in Table I lists $(\gamma_p - \beta_p)/2$, which should be equal to γ for both models. Again the fit for $d \geq 3$ is reasonable. The apparent disagreements at $d \geq 6$

TABLE I. Exponent estimates from Dlog Padé analysis.

d	p_c	γ_{DAFF}	γ_{DRFIM}	$\frac{1}{2}(\gamma_p - \beta_p)$[a]
1	1[b]	1[b]	$\frac{1}{2}$[b]	$\frac{1}{2}$[b]
2	$\frac{1}{2}$[b]	1.25 ± 0.10	0.7 ± 0.2	$\frac{9}{8}$[b]
3	0.247	0.59 ± 0.15	0.58 ± 0.1	0.65
4	0.160	0.43 ± 0.05	0.34 ± 0.03	0.5
5	0.118	0.27 ± 0.04	0.20 ± 0.02	0.25
6	0.094	0.22 ± 0.07	0.13 ± 0.05	$(\ln)^{9/7}$[b]
7	0.079	0.15 ± 0.05	0.12 ± 0.04	$(\ln)$[b]
8	0.068	0.15 ± 0.15	0.10 ± 0.04	$(\ln)$[b]

[a]Values for $d = 3,4,5$ taken from Ref. 17.
[b]Exact results.

probably indicate that our approximation procedure does not adequately allow for the predicted logarithmic corrections. (From the results of Ref. 25, one sees that logarithmic factors may easily change the exponents by ~ 0.1.) It is interesting to note that for $d > 2$, the effective values for γ_{DAFF} are consistently larger than those for γ_{DRFIM} and closer to the predicted value $(\gamma_p - \beta_p)/2$. Both series probably exhibit effective exponents which would more nearly approach the predicted values if the series were longer.

The results at $d = 2$ seem to be different: γ_{DRFIM} seems to be significantly smaller than both the value we obtain for γ_{DAFF} and the predicted value. If we believe that for all $d > 1$ the unit cells which have unequal numbers of occupied sites on the two sublattices have a finite concentration, then we must conclude that the asymptotic behavior of the two models is the same. In this case, the apparent difference between the two results implies an extremely slow crossover for the DRFIM. It would be useful to test this idea by other methods, e.g., Monte Carlo simulations. The alternative is even more stimulating: Could the two models really be different at $d = 2$? We leave this question for future studies. (See note added in proof.)

VIII. CONCLUSIONS

Based on scaling arguments and numerical evidence we have concluded that at low temperature and random fields (uniform field on the DAFF) the ordering susceptibility diverges as $(p_c - p)^{-\gamma}$, with $\gamma_{\text{DAFF}} = \gamma_{\text{DRFIM}} = (\gamma_p - \beta_p)/2$, which is different from the zero-field value, γ_p. For $d = 2$, either the crossover to this behavior is very slow or the two models have different critical behavior. (See note added in proof.)

Crossover to finite fields was shown to have novel features, and the behavior of χ at fixed p probably crosses over from $(p_c - p)^{-\gamma}$ to $h^{-(\gamma_p - \beta_p)/(\gamma_p + \beta_p)}$ [see Eq. (3.5)]. At $d = 3$, the power of h is 0.62, which is very different from the power 2 expected[4] at T_c. At $d = 2$ the new power is 0.89. A similar crossover is predicted for the structure factor, changing from $(p_c - p)^{-\gamma_p}$ to $h^{-2\gamma_p/(\gamma_p + \beta_p)}$, with the new power equal to 1.89 at $d = 2$ and to 1.6 at $d = 3$ (instead of[4] 2 for both dimensions). These predictions should be observable both in computer and in real experiments. We hope that these results will

stimulate more detailed studies of dilute RFIM and DAFF systems.

Note added in proof. A recent refinement in our analysis is consistent with $\gamma_{\text{DRFIM}} = \gamma_{\text{DAFF}}$ for $d = 0$.

APPENDIX A: POTTS MODEL AND SITE-OCCUPATION DISTRIBUTIONS

In this appendix we show the relation between the partition function for the Potts model in uniform and staggered fields, denoted h and h_s, respectively, and the distribution function for the average number of clusters, $W(n_A, n_B, p)$ consisting of n_A A sites and n_B B sites, at concentration p. This formulation is a generalization of that previously given by Stephen[19] and Harris and Lubensky[20] for the distribution function regarded as a function of p and the *total number* of sites in a cluster.

For a Potts model with ferromagnetic coupling J between nearest-neighboring sites, the partition function Z is

$$Z = \underset{\{\mathbf{v}(\mathbf{x})\}}{\text{Tr}} \prod_{\text{bonds}} \exp[J\mathbf{v}(\mathbf{x}) \cdot \mathbf{v}(\mathbf{x}')]$$
$$\times \prod_{\text{sites}} \exp[h(\mathbf{x})(s-1)\mathbf{v}(\mathbf{x}) \cdot \hat{\mathbf{e}}_1] , \quad \text{(A1)}$$

where $\mathbf{v}$ is one of the s unit vectors, $\hat{\mathbf{e}}_1, \hat{\mathbf{e}}_2, \ldots, \hat{\mathbf{e}}_s$, which points from the center of an $(s-1)$-dimensional simplex to any of its s vertices, $h(\mathbf{x})$ is the field in the $\hat{\mathbf{e}}_1$ direction acting on site $\mathbf{x}$, $\text{Tr}_{\{\mathbf{v}(\mathbf{x})\}}$ indicates a trace over all states of the Potts vectors, and we have taken the thermal energy kT to be unity.

We now use the identity

$$e^{J\mathbf{v}(\mathbf{x}) \cdot \mathbf{v}(\mathbf{x}')} = e^{(s-1)J}[e^{-sJ} + (1 - e^{-sJ})\delta_{\mathbf{v}(\mathbf{x}), \mathbf{v}(\mathbf{x}')}] , \quad \text{(A2)}$$

where δ is unity if its two subscripts coincide and is zero otherwise. We set $\exp(-sJ) = p$,

$$Z = e^{(s-1)JNz/2} \underset{\{\mathbf{v}(\mathbf{x})\}}{\text{Tr}} \prod_{\text{bonds}} [1 - p + p\delta_{\mathbf{v}(\mathbf{x}), \mathbf{v}(\mathbf{x}')}]$$
$$\times \prod_{\text{sites}} e^{h(\mathbf{x})(s-1)\mathbf{v}(\mathbf{x}) \cdot \hat{\mathbf{e}}_1} , \quad \text{(A3)}$$

where z is the coordination number of the lattice. We now expand the product over bonds in powers of $1-p$ and $p\delta$, and identify each term in this expansion with a configuration C, in which $1-p$ corresponds to a vacant bond and $p\delta$ to an occupied bond. For each configuration C, we classify sites into clusters Γ of one or more sites connected directly or indirectly via occupied bonds. Note that because of the delta functions all sites in the same cluster Γ have the same Potts vector, $\mathbf{v}_\Gamma$. Thus, we have

$$Z = e^{(s-1)JNz/2} \sum_C P(C) \, \underset{\{v_\Gamma\}}{\mathrm{Tr}} \, \prod_{\Gamma \in C} \exp \left[\sum_{x \in \Gamma} h(\mathbf{x})(s-1)\mathbf{v}_\Gamma \cdot \hat{\mathbf{e}}_1 \right] . \tag{A4}$$

Here $P(C)$ is the percolation weight for the configuration C, i.e., it is the product of a factor p or $1-p$ for each bond depending on whether it is occupied or vacant, respectively, and $\Gamma \in C$ indicates that the product is taken over all clusters in the configuration C.

We now set $h(\mathbf{x})$ equal to h_A for $\mathbf{x}$ on the A sublattice and h_B for $\mathbf{x}$ on the B sublattice, and let $n_A(\Gamma)$ and $n_B(\Gamma)$ denote the number of sites the cluster Γ has on the A and B sublattices, respectively. Then we can write the trace over the Potts vectors in Eq. (A4) as

$$Z = e^{(s-1)JNz/2} \sum_C P(C) \prod_{\Gamma \in C} \left[e^{(s-1)[h_A n_A(\Gamma) + h_B n_B(\Gamma)]} + (s-1)e^{-[h_A n_A(\Gamma) + h_B n_B(\Gamma)]} \right] . \tag{A5}$$

In the limit $s \to 1$, we have to lowest nontrivial order in $s-1$

$$Z = 1 + NzJ(s-1)/2 + N(s-1)(h_A + h_B)/2 + (s-1) \sum_C P(C) \sum_{\Gamma \in C} e^{-[h_A n_A(\Gamma) + h_B n_B(\Gamma)]} . \tag{A6}$$

In the limit $s \to 1$ we therefore have

$$\frac{\ln Z}{(s-1)N} = zJ/2 + (h_A + h_B) + \sum_{n_A, n_B} W(n_A, n_B, p) e^{-(h_A n_A + h_B n_B)} . \tag{A7}$$

Therefore we write

$$W(n_A, n_B, p) = - \int_{a-i\infty}^{a+i\infty} \frac{dh_A}{2\pi i} \int_{a-i\infty}^{a+i\infty} \frac{dh_B}{2\pi i} f(h_A, h_B, p) e^{n_A h_A + n_B h_B} , \tag{A8}$$

where $-f$ is defined to be the left-hand side of Eq. (A7).

In analogy with the antiferromagnet in uniform and staggered fields, we may write a Landau free-energy functional F (the minimum of which gives f) in terms of uniform and staggered densities, M and M_s, respectively:

$$F = \tfrac{1}{2}rM^2 + \frac{1}{2\chi_s}M_s^2 + \tfrac{2}{3}w(M^3 + 3MM_s^2)$$
$$- \tfrac{1}{2}(h_A + h_B)M - \tfrac{1}{2}(h_A - h_B)M_s , \tag{A9}$$

where $r \sim (p_c - p)$, χ_s is a staggered percolative susceptibility (and is of order unity), $w \sim 1$, and we have omitted higher-than-cubic terms. Note that the $s=1$ state Potts model has a characteristic *local* cubic term $w\psi^3/3$ in its Landau free energy, which in this case becomes $w[(M + M_s)^3 + (M - M_s)^3]$ for a two-sublattice representation. Minimization of Eq. (A9) with respect to M_s yields

$$F = \tfrac{1}{2}rM^2 + \tfrac{2}{3}wM^3 - \tfrac{1}{2}(h_A + h_B)M$$
$$- \tfrac{1}{8}(h_A - h_B)^2 \frac{\chi_s}{1 + 4wM\chi_s} . \tag{A10}$$

For small M we may write this as

$$F = -\tfrac{1}{8}\chi_s(h_A - h_B)^2 - \tilde{h}M + \tfrac{1}{2}\tilde{r}M^2 + \tfrac{2}{3}\tilde{w}M^3 , \tag{A11}$$

where the renormalized coupling constants are

$$\tilde{h} = (h_A + h_B)/2 - \tfrac{1}{2}(h_A - h_B)^2 w\chi_s^2 , \tag{A12a}$$

$$\tilde{r} = r - 4(h_A - h_B)^2 w^2 \chi_s^3 , \tag{A12b}$$

$$\tilde{w} = w + 12(h_A - h_B)^2 w^3 \chi_s^4 . \tag{A12c}$$

Now minimization with respect to M yields the usual[19,20] mean-field result:

$$f \sim \frac{\tilde{r}^3}{48\tilde{w}^2} + \frac{1}{4}\frac{\tilde{r}\tilde{h}}{\tilde{w}} - \frac{1}{48\tilde{w}^2}(\tilde{r}^2 + 8\tilde{w}\,\tilde{h})^{3/2} . \tag{A13}$$

Only the last term is important in evaluating Eq. (A8):

$$W(n_A, n_B, p) = \int_{a-i\infty}^{a+i\infty} \frac{dh}{2\pi i} \int_{a-i\infty}^{a+i\infty} \frac{dh_s}{2\pi i} e^{n_A(h+h_s) + n_B(h-h_s)} \frac{2}{48\tilde{w}^2} [\tilde{r}^2 + 8\tilde{w}(h - h_s^2 w\chi_s^2)]^{3/2} , \tag{A14}$$

where we introduced $h = (h_A + h_B)/2$ and $h_s = (h_A - h_B)/2$. To evaluate this integral, it is convenient to integrate first over h, then over h_s, and in the latter integral to keep only terms in the exponential up to order h_s^2, as is justified for p near p_c. Writing $n = n_A + n_B$ and $n_s = n_A - n_B$, we have

$$W(n_A, n_B, p) = (8w\pi)^{-1/2} n^{-5/2} e^{-nr^2/8w}$$
$$\times (4\pi n w\chi_s^2)^{-1/2} e^{-n_s^2/4nw\chi_s^2} . \tag{A15}$$

This result indicates that the configurational average of n_s^2 has the same singularity as that of n, in agreement

with the heuristic argument of Sec. III.

Deviations from the mean-field result can be obtained by adding the fluctuation term, $(\nabla M)^2$, and deriving an ϵ expansion.[19,20] Since we expect fluctuations only in M, and *not* in the antiferromagnetic order parameter, M_s, we can still minimize with respect to M_s, and end up with the effective Hamiltonian of Eq. (A11). Thus, h is shifted into $h - h_s^2 w \chi_s^2$, and h_s^2 scales in the same way as h. This

observation immediately implies that n_s^2 scales as n, leading to

$$W(n_A, n_B; p)/W(n; p) \sim n^{-1/2} g(n_s^2/n) , \tag{A16}$$

where g is some scaling function. For $n_s = 0$ we therefore have

$$W(n, n; p)/W(n; p) \sim n^{-1/2} .$$

APPENDIX B: TABULATION OF SERIES COEFFICIENTS

In this appendix we give explicit expressions for the series for χ for both models considered in powers of p up to terms of order p^{11}. The coefficient of p^n for general spatial dimension d is a polynomial of order n in the variable d. We give the results in terms of rational fractions except where the denominators are excessively large:

$$\chi_{\text{DRFIM}} = dp + (-4d^2 + 2d)p^2 + (32d^3 - 37d^2 + 10\tfrac{1}{2}d)p^3 + (-202\tfrac{2}{3}d^4 + 384d^3 - 228\tfrac{1}{12}d^2 + 37\tfrac{3}{4}d)p^4$$

$$+ (1318\tfrac{2}{3}d^5 - 3499\tfrac{1}{3}d^4 + 3174\tfrac{1}{12}d^3 - 971\tfrac{1}{24}d^2 - 8\tfrac{1}{2}d)p^5$$

$$+ (-8536\tfrac{8}{15}d^6 + 29\,322\tfrac{2}{3}d^5 - 36\,282\tfrac{2}{3}d^4 + 16\,798\tfrac{1}{12}d^3 + 233\tfrac{23}{40}d^2 - 1553\tfrac{7}{8}d)p^6$$

$$+ (55\,724\tfrac{4}{5}d^7 - 235\,422\tfrac{2}{5}d^6 + 371\,212\tfrac{2}{3}d^5 - 236\,308\tfrac{1}{2}d^4 + 8486\tfrac{8}{15}d^3 + 49\,958\tfrac{2}{3}d^2 - 13\,626\tfrac{13}{16}d)p^7$$

$$+ (-365\,966\tfrac{198}{315}d^8 + 1\,837\,868\tfrac{4}{15}d^7 - 3\,540\,361\tfrac{3}{5}d^6 + 2\,932\,470d^5 - 404\,195\tfrac{227}{240}d^4 - 866\,158\tfrac{17}{40}d^3$$

$$+ 457\,518\tfrac{2581}{3360}d^2 - 51\,205\tfrac{19}{32}d)p^8$$

$$+ (2\,418\,917\tfrac{309}{315}d^9 - 14\,086\,863\tfrac{207}{315}d^8 + 32\,173\,579\tfrac{23}{30}d^7 - 33\,293\,777\tfrac{4}{5}d^6$$

$$+ 9\,177\,209\tfrac{23}{320}d^5 + 10\,622\,089\tfrac{191}{320}d^4 - 8\,816\,243\tfrac{11773}{26880}d^3 + 1\,777\,508\tfrac{3403}{8960}d^2 + 27\,617\tfrac{203}{384}d)p^9$$

$$+ (-16\,079\,028\tfrac{28}{81}d^{10} + 106\,583\,223\tfrac{1971}{2835}d^9 - 282\,281\,319\tfrac{447}{567}d^8 + 353\,670\,919\tfrac{11}{30}d^7$$

$$- 153\,584\,184\tfrac{38661}{45360}d^6 - 99\,606\,156\tfrac{199}{240}d^5 + 130\,225\,810\tfrac{10087}{36288}d^4 - 40\,449\,928\tfrac{8961}{10080}d^3$$

$$+ 2\,114\,504\tfrac{4279}{5040}d^2 - 593\,883\tfrac{25}{32}d)p^{10}$$

$$+ (107\,429\,661.227\,795d^{11} - 798\,875\,277.237\,390d^{10} + 2\,411\,563\,242.556\,614d^9$$

$$- 3\,568\,756\,734.735\,450d^8 + 2\,157\,951\,873.168\,704d^7 + 669\,075\,986.194\,676d^6$$

$$- 1\,642\,452\,721.525\,226d^5 + 782\,381\,724.776\,800d^4 - 180\,853\,801.627\,106d^3$$

$$+ 92\,960\,921.184\,958d^2 - 30\,424\,822.058\,594d)p^{11} , \tag{B1}$$

$$\chi_{\text{DAFF}} = 2dp + (-8d^2 + 4d)p^2 + (64d^3 - 68d^2 + 18d)p^3 + (-405\tfrac{1}{3}d^4 + 720d^3 - 388\tfrac{2}{3}d^2 + 50d)p^4$$

$$+ (2637\tfrac{1}{3}d^5 - 6626\tfrac{2}{3}d^4 + 5572\tfrac{2}{3}d^3 - 1407\tfrac{1}{3}d^2 - 134d)p^5$$

$$+ (-17\,073\tfrac{1}{15}d^6 + 55\,973\tfrac{1}{3}d^5 - 65\,085\tfrac{1}{3}d^4 + 26\,486\tfrac{2}{3}d^3 + 2532\tfrac{2}{5}d^2 - 2894d)p^6$$

$$+ (111\,449d^7 - 452\,082\tfrac{2}{15}d^6 + 676\,626\tfrac{2}{3}d^5 - 392\,761\tfrac{1}{3}d^4 - 10\,566\tfrac{4}{15}d^3 + 85\,527\tfrac{7}{15}d^2 - 18\,108d)p^7$$

$$+ (-731\,933\tfrac{9}{35}d^8 + 3\,545\,800\tfrac{8}{15}d^7 - 6\,531\,637\tfrac{1}{3}d^6 + 5\,045\,530\tfrac{2}{3}d^5 - 453\,753\tfrac{3}{5}d^4 - 1\,452\,655\tfrac{1}{5}d^3$$

$$+ 611\,290\tfrac{4}{21}d^2 - 32\,754d)p^8$$

$$+ (4\,837\,835\tfrac{101}{105}d^9 - 27\,279\,353\tfrac{47}{105}d^8 + 59\,915\,847\tfrac{1}{5}d^7 - 58\,651\,406\tfrac{2}{5}d^6 + 13\,846\,800\tfrac{19}{30}d^5 + 17\,836\,889\tfrac{2}{5}d^4$$

$$- 12\,207\,801\tfrac{9}{70}d^3 + 1\,599\,588\tfrac{47}{105}d^2 + 101\,745\tfrac{1}{3}d)p^9$$

$$+ (-32\,158\,056\tfrac{392}{567}d^{10} + 2\,070\,284\,766\tfrac{106}{315}d^9 - 529\,613\,430\tfrac{26}{945}d^8 + 633\,680\,168d^7 - 252\,461\,644\tfrac{238}{945}d^6$$

$$- 169\,507\,946\tfrac{11}{15}d^5 + 189\,402\,713\tfrac{109}{405}d^4 - 48\,377\,047\tfrac{38}{63}d^3 + 5\,721\,775\tfrac{221}{315}d^2 - 37\,151\,789d)p^{10}$$

$$+ (214\,859\,322\tfrac{6458}{14175}d^{11} - 1\,555\,668\,033\tfrac{1949}{2835}d^{10} + 4\,552\,016\,240\tfrac{40}{189}d^9 - 6\,476\,161\,246\tfrac{538}{945}d^8$$

$$+ 3\,691\,082\,077\tfrac{329}{675}d^7 + 1\,165\,933\,236\tfrac{49}{136}d^6 - 2\,509\,806\,737\tfrac{877}{1134}d^5 + 1\,130\,369\,735\tfrac{2579}{2835}d^4$$

$$- 407\,614\,858\tfrac{1201}{3150}d^3 + 251\,857\,235\tfrac{62}{63}d^2 - 56\,866\,750d)p^{11} . \tag{B2}$$

[1]For recent theoretical reviews, see A. Aharony, in *Multicritical Phenomena,* edited by R. Pynn and A. Skjeltorp (Plenum, New York, 1984); Y. Imry, J. Stat. Phys. **34**, 849 (1984).

[2]Y. Imry and S.-k. Ma, Phys. Rev. Lett. **35**, 1399 (1975).

[3]G. Grinstein and S.-k. Ma, Phys. Rev. B **28**, 2588 (1983), and references therein.

[4]A. Aharony and E. Pytte, Phys. Rev. B **27**, 5872 (1983).

[5]G. Grinstein and J. F. Fernandez, Phys. Rev. B **29**, 6389 (1984).

[6]J. Villain, Phys. Rev. Lett. **52**, 1543 (1984); R. Bruinsma and G. Aeppli, Phys. Rev. Lett. **52**, 1547 (1984).

[7]S. Fishman and A. Aharony, J. Phys. C **12**, L729 (1979).

[8]P.-z. Wong, S. von Molnar, and P. Dimon, J. Appl. Phys. **53**, 7954 (1982); Solid State Commun. **48**, 573 (1983).

[9]M. Hagen, R. A. Cowley, G. Shirane, R. J. Birgeneau, and H. J. Guggenheim, Phys. Rev. B **28**, 2602 (1983).

[10]J. Cardy, Phys. Rev. B **29**, 505 (1984).

[11]For a recent review, see R. J. Birgeneau, R. A. Cowley, G. Shirane, and H. Yoshizawa, J. Stat. Phys. **34**, 817 (1984).

[12]A. Aharony, Phys. Rev. B **18**, 3318 (1978).

[13]Y. Gefen, A. Aharony, Y. Shapir, and A. N. Berker, J. Phys. C **15**, L801 (1982).

[14]I. Morgenstern, K. Binder, and R. M. Hornreich, Phys. Rev. B **23**, 287 (1981).

[15]P.-z. Wong and J. W. Cable, Phys. Rev. B **28**, 5361 (1983).

[16]A. R. King, V. Jaccarino, T. Sakskibara, M. Motokawa, and M. Date, Phys. Rev. Lett. **47**, 117 (1981).

[17]See, e.g., D. Stauffer, Phys. Rep. **54**, 3 (1979).

[18]I. S. Gradshteyn and I. M. Ryzhik, *Table of Integrals, Series, and Products* (Academic, New York, 1965).

[19]M. J. Stephen, Phys. Rev. B **15**, 5674 (1977).

[20]A. B. Harris and T. C. Lubensky, Phys. Rev. B **24**, 2656 (1981).

[21]T. C. Lubensky and J. Isaacson, Phys. Rev. A **20**, 2130 (1979).

[22]A. B. Harris and S. Kirkpatrick, Phys. Rev. B **16**, 542 (1977).

[23]M. E. Fisher and J. W. Essam, J. Math. Phys. **2**, 609 (1961).

[24]A. Kapitulnik, Y. Gefen, and A. Aharony, J. Stat. Phys. (to be published).

[25]R. Fisch and A. B. Harris, Phys. Rev. Lett. **35**, 798 (1977).